



# Abaloparatide increases bone mineral density and bone strength in ovariectomized rabbits with glucocorticoid-induced osteopenia

H. Chandler<sup>1</sup> · D.J. Brooks<sup>2</sup> · G. Hattersley<sup>1</sup> · M.L. Bouxsein<sup>2,3</sup> · B. Lanske<sup>1</sup>

Received: 4 March 2019 / Accepted: 21 April 2019 / Published online: 3 May 2019  
© The Author(s) 2019

## Abstract

**Summary** Glucocorticoid (GC) therapy is the commonest cause of secondary osteoporosis. Ovariectomized rabbits receiving the GC methylprednisolone for 6 weeks exhibited relatively lower vertebral and femoral bone mass. Treatment with the PTH receptor agonist abaloparatide for 12 weeks during ongoing methylprednisolone administration increased cortical and trabecular bone mass and femur bending strength.

**Introduction** Abaloparatide, an osteoanabolic PTHrP analog, increases bone mineral density (BMD) and reduces fracture risk in women with postmenopausal osteoporosis. This study assessed abaloparatide effects on BMD and bone strength in ovariectomized (OVX) rabbits with glucocorticoid (GC)-induced osteopenia.

**Methods** Thirty-two rabbits underwent OVX and 8 underwent sham surgery. One day later, 24 OVX rabbits began daily s.c. GC injections (methylprednisolone, 1 mg/kg/day) for 6 weeks, while 8 OVX and 8 sham controls received no GC. GC-challenged rabbits (8/group) then received GC (0.5 mg/kg/day) along with daily s.c. vehicle (GC-OVX), abaloparatide 5 µg/kg/day (ABL5), or 25 µg/kg/day (ABL25) for 12 weeks, and the no-GC OVX and sham controls received daily vehicle.

**Results** GC-OVX rabbits showed significant deficits in vertebral and proximal femur areal BMD, lower cortical area, thickness and volumetric BMD of the femur diaphysis, and reduced trabecular bone volume and volumetric BMD in the vertebra and distal femur versus sham controls. These deficits were significantly reversed in the ABL25 group, which also showed enhanced trabecular micro-architecture versus GC-OVX controls. Destructive bending tests showed significantly lower femur diaphysis ultimate load and bending rigidity of the femoral diaphysis in the GC-OVX group versus sham controls, whereas these parameters were similar in the ABL25 group vs sham controls.

**Conclusions** Abaloparatide 25 µg/kg/day mitigated the adverse effects of GC administration on cortical and trabecular bone and improved femoral strength in OVX rabbits. These results suggest potential promise for abaloparatide as an investigational therapy for glucocorticoid-induced osteoporosis.

**Keywords** Bone biomechanics · Cortical bone · Corticosteroid · Osteoporosis · Trabecular architecture

## Introduction

Glucocorticoid (GC)-induced osteoporosis (GIOP) is the most common secondary form of osteoporosis. Bone loss can be

particularly rapid during the first few months after initiating GC therapy [1, 2]. This effect, combined with adverse effects of GC therapy on bone matrix quality and the tendency for GC therapy to increase the risk of falls, can lead to a near-immediate increase in fracture risk after initiating GC therapy [1]. GCs promote bone loss by increasing bone resorption and inhibiting bone formation [1, 2], leading to the deterioration of trabecular bone volume and architecture [3]. GCs also cause cortical bone loss by increasing endocortical osteoclasts [4] and by increasing cortical porosity [5].

The pathogenesis of GIOP is clearly multifactorial, and the suppression of parathyroid hormone-related protein (PTHrP) expression represents one potential mechanism by which GCs may lead to impaired bone formation. PTHrP is an important

✉ B. Lanske  
blanske@radiuspharm.com

<sup>1</sup> Radius Health Inc., 950 Winter Street, Waltham, MA 02451, USA

<sup>2</sup> Center for Advanced Orthopaedic Studies, Beth Israel Deaconess Medical Center, Boston, MA, USA

<sup>3</sup> Department of Orthopedic Surgery, Harvard Medical School, Boston, MA, USA

endogenous anabolic factor that maintains bone formation [6, 7], and cell culture and animal studies indicate that GCs reduce PTHrP expression by osteoblasts and other cell types [8–10]. GCs can also sharply upregulate expression of the PTH/PTHrP receptor [9], which may foster responsiveness of the GC-exposed skeleton to the osteogenic effects of PTHrP and other PTH receptor agonists. Indeed, clinical and preclinical studies show that PTH/PTHrP receptor agonists including PTHrP and teriparatide (TPTD) promote bone formation and increase bone mass in GIOP settings [10–12]. The PTHrP analog abaloparatide increases bone formation and bone mass and reduces fracture risk in women with postmenopausal osteoporosis, with modest increases in bone resorption [13, 14]. Preclinical studies in GC-naïve estrogen-deficient (ovariectomized; OVX) and androgen-deficient (orchiectomized) animals indicate that abaloparatide increases bone formation, bone mass, and bone strength without increasing bone resorption [15–19]. These pharmacodynamic properties suggest that abaloparatide may increase BMD and bone strength in animals and perhaps patients with GC-induced bone loss, but the skeletal effects of abaloparatide have not been previously assessed in patients with GIOP or in GC-challenged animals. The current study evaluated the effects of 12 weeks of abaloparatide therapy on bone mass and bone strength in adult OVX rabbits with GC-induced bone loss.

## Materials and methods

### Animal care, surgery, and dual X-ray absorptiometry

All animal procedures and activities were approved by and performed in an AAALAC-accredited vivarium at PharmaLegacy Laboratories (Shanghai, China). A total of 44 female New Zealand White rabbits (including 4 spares) aged 5–7 months and weighing between 3 and 4 kg were obtained from Qingdao Kangda Biotechnology (Shangdon Province, China). Animals underwent health inspections upon arrival and received ear tattoos for individual identification. Animals were acclimated in individual stainless-steel cages (81.5 cm × 50 cm × 34 cm) for at least 7 days in a vivarium with a temperature range of 16–26 °C, relative humidity of 40–70%, and a 12-h light/dark cycle. Animals had free access to irradiated rabbit food (Shanghai SLAC Laboratory Animal Co. Ltd. China) and municipal tap water filtered with a Mol Ultrapure Water System.

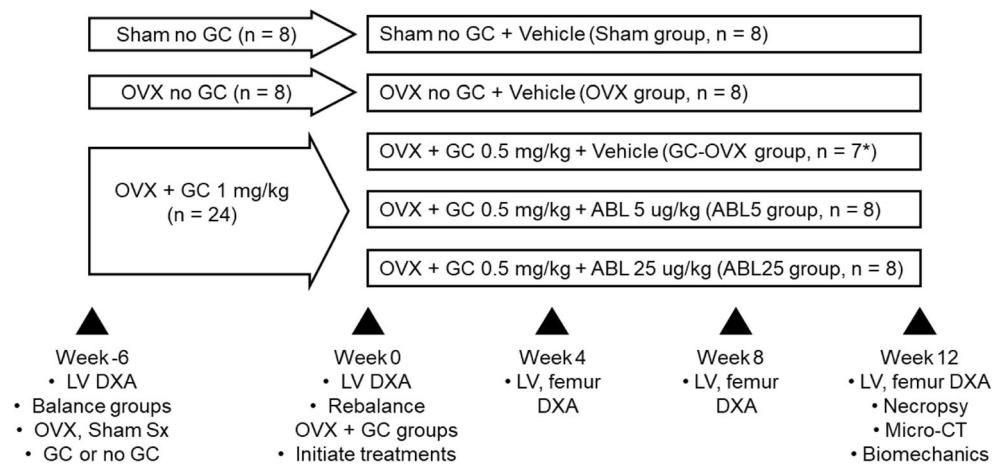
A study design schema is presented in Fig. 1. Six weeks prior to treatment initiation, all animals underwent dual-energy X-ray absorptiometry (DXA; Hologic Discovery, Marlborough, MA, USA) of the L2–L5 lumbar vertebrae (LV) after pre-anesthesia with zolazepam (Zoletil, 10–15 mg/kg i.m.; Virbac, Belgium) and anesthesia with 1.5–

3% isoflurane in oxygen. LV DXA areal bone mineral density (aBMD) data were used to allocate the 40 study animals into 2 initial groups of 32 and 8 animals that were balanced for average LV aBMD and body weight. The group of 32 rabbits underwent OVX surgery while the group of 8 rabbits underwent sham surgery. For surgery, all animals received atropine (0.2 mg/kg i.m.) and were pre-anesthetized with zolazepam i.m. (10–15 mg/kg), with anesthesia maintained with 1.5–3% isoflurane in oxygen. The abdominal fur was shaved off and the peritoneal cavity was accessed via a 2–3-cm skin incision. Subcutaneous tissue was bluntly separated to expose each ovary, followed by ligation of the fallopian tubes and removal of both ovaries with a scalpel. The abdominal wall and overlying skin were then sequentially sutured closed. Sham surgery was similar but without the tubal ligation and ovary removal steps. All animals received an i.m. dose of antibiotic (gentamycin, 20 mg/kg) on the day of surgery, and post-surgical buprenorphine (0.05 mg/kg i.m.) was administered for pain control. One day after surgery, 24 of the OVX rabbits started received daily s.c. injections of the GC methylprednisolone at 1 mg/kg/day (Pfizer Manufacturing Belgium NV), while the remaining 8 OVX animals and the 8 sham controls did not receive GC.

A 6-week bone depletion period was then implemented to allow the effects of OVX and GC to manifest. LV DXA was performed again on all animals, and the 24 GC-treated OVX rabbits were divided into 3 groups of 8 animals based on similar average LV aBMD and body weight. All 24 GC-treated OVX rabbits continued to receive GC at a dose of 0.5 mg/kg/day (GC dose reduction was to mitigate the risk of further weight loss), and treatments were initiated with daily s.c. vehicle (Veh) (0.9% sterile sodium chloride for injection USP; GC-OVX group) or with abaloparatide (ABL) (Radius Health, Waltham, MA, USA) at 5 µg/kg (ABL5 group) or 25 µg/kg (ABL25 group) (all  $n = 8$ ; Fig. 1). The remaining 8 OVX rabbits (OVX group) and 8 sham controls (Sham group) received s.c. vehicle (Fig. 1).

Additional DXA scans of LV and the right proximal femur were performed on anesthetized animals at weeks 4, 8, and 12 of the treatment period and animals were then sacrificed by an overdose of zolazepam followed by exsanguination. At necropsy, the uterus was removed from all animals and weighed wet. Blood was collected from the sham and OVX groups and prepared as serum for estradiol measurements. Estradiol was measured by ELISA (Catalog #KGE014, R&D Systems China Co, Shanghai); the assay had lower quantitation limit of 18.4 pmol/L, and this value was imputed for all samples found to be below this detection limit, which comprised 5 of the 8 animals in OVX group and none in the sham group. The 4th lumbar vertebra (L4) and the right femur were collected and stored at –20 °C for high-resolution structural analyses and biomechanical testing.

**Fig. 1** Study design and procedures. GC, glucocorticoid (methyl-prednisolone); OVX, ovariectomy; ABL, abaloparatide; DXA, dual X-ray absorptiometry; LV, lumbar vertebrae. \*GC-OVX group had an N of 7 due to one animal death during the bone depletion period



## Micro-computed tomography

After removing the proximal end, the right femur was scanned with a high-resolution desktop micro-CT imaging system ( $\mu$ CT40, Scanco Medical AG, Bruttisellen, Switzerland). The L4 vertebral body was isolated by removing the transverse and spinous processes with a low-speed diamond saw (IsoMet 1000, Buehler, Lake Bluff, Illinois, USA) and scanned using the same micro-CT system. Scans were acquired using a  $15\text{-}\mu\text{m}^3$  isotropic voxel size, with 70-kVp peak x-ray tube potential, 114-mAs tube current, and 200-ms integration time and subjected to Gaussian filtration and segmentation. Image acquisition and analysis protocols adhered to published guidelines for the assessment of rodent bones by micro-CT [20].

Cortical bone density and architectural parameters were assessed in a 2-mm-long region of the femoral mid-diaphysis. Cortical bone was identified using a segmentation threshold of  $700\text{ mg hydroxyapatite}/\text{cm}^3$ . Variables measured included total cross-sectional area (Tt.Ar; bone + medullary area), cortical bone area (Ct.Ar), marrow (medullary) area (Ma.Ar), cortical bone area fraction (Ct.Ar/Tt.Ar), cortical volumetric bone mineral density (Ct.vBMD), cortical tissue mineral density (Ct.TMD), cortical thickness (Ct.Th), and cortical porosity (Ct.Po).

Trabecular bone was analyzed in the L4 vertebral body and distal right femur. The trabecular region of interest (ROI) for the distal femur begins 1.5 mm superior to the junction of the medial and lateral condyles and extends proximally 2 mm (133 slices) (Fig. 4). This ROI comprises epiphyseal bone, which is a preferred region for trabecular analyses in skeletally mature New Zealand White rabbits based on more robust trabecular architecture compared with the trabecular-poor metaphyseal region [21]. The trabecular ROI for L4 begins at a point that is 1/8th of the vertebral body's height superior to the caudal end-plate and extends proximally 2 mm (133 slices) (Fig. 4). At both skeletal sites, the trabecular bone region was identified by semi-manually contouring the trabecular bone in

the ROI with the assistance of an auto-thresholding software algorithm. A threshold of  $450\text{ mg hydroxyapatite}/\text{cm}^3$  was used to segment bone from soft tissue in all groups. Morphometric variables were computed from the binarized images using direct 3D techniques that do not rely on any prior assumptions about the underlying structure. Trabecular parameters included trabecular bone volume per total volume (Tb.BV/TV), trabecular bone mineral density (Tb.BMD), trabecular thickness (Tb.Th), trabecular number (Tb.N), trabecular separation (Tb.Sp), connectivity density (Conn.D), and structure model index (SMI). SMI describes the plate-vs-rod-like nature of the architecture, with high SMI values indicating rod-like structures and low values characterizing plate-like structures. In addition to L4 trabecular analyses, an entire cross-section of the vertebral body was analyzed in an 8-mm-long region at the middle of its longitudinal axis (Fig. 4). A contour was manually drawn around the outer L4 body surface and the entire cross-section was segmented using a threshold of  $450\text{ mg hydroxyapatite}/\text{cm}^3$  for analysis of bone volume, total volume, BV/TV, vBMD, and TMD.

## Bone biomechanics

Following micro-CT scanning, the proximal and distal ends of the femur were removed with a low-speed diamond saw. The resulting 40-mm-long section of the femoral diaphysis was tested in three-point bending using a servo-hydraulic material testing machine (Model 8511, Instron, Norwood, MA). The test was performed with the cranial surface of the femur resting on bottom supports 30 mm apart with the mid-diaphysis at the central load point, where load was applied at a rate of 2 mm/min until failure, with force and displacement data collected at 50 Hz. Ultimate load, bending rigidity, and work (energy) to ultimate load were calculated based on the force and displacement data. Work to ultimate load comprised the area under the force-displacement curve as measured using the Riemann Sum method. Bending rigidity was calculated using the linear portion of the force-displacement curve.

The L4 vertebral body was prepared for biomechanical testing by removing the end plates and posterior and transverse elements with the low-speed diamond saw, producing samples with a uniform height (8 mm) and plano-parallel ends. The vertebral bodies were then loaded in compression between flat platens of the material testing machine at a rate of 2 mm/min. Force and displacement data were used to measure the ultimate load, stiffness, and work to ultimate load for each sample.

## Statistical analyses

Serum estradiol data for the sham and OVX group were compared by *t* test. Uterine weight and micro-CT data were evaluated by one-way ANOVA, followed when significant by Tukey's post-test comparing all groups with each other. DXA data were evaluated by two-way ANOVA, followed when significant by Tukey's post-test comparing each group within each time point. Linear regressions within individual groups were analyzed for goodness of fit (*r* value), and *r* values for all groups combined were reported when there were no significant between-group differences for slopes, elevations, or Y-intercepts. Statistical analyses were performed using GraphPad Prism V8.0, with a *P* value of <0.05 used to indicate statistically significant differences.

## Results

### General animal observations

One of the 24 animals that underwent OVX surgery plus GC administration died during the bone depletion period. All data for that animal were excluded, leaving the GC-OVX group with a sample size of 7. All other animals survived to scheduled necropsy. The OVX group showed modestly and non-significantly lower body weight throughout the study compared with sham controls (Fig. 2a). The GC-OVX group had significantly lower body weight compared with sham controls and OVX controls starting at week -4 and week -3, respectively, and persisting through the rest of the study. There were no significant body weight differences between the GC-OVX, ABL5, and ABL25 groups at any time point (Fig. 2a). Abaloparatide treatment was well tolerated based on body weight findings and twice-daily animal inspections. Success of OVX surgery was confirmed based on average uterus weights being 76–83% lower in the four OVX groups compared with sham controls (all *P* < 0.001; data not shown), and by average serum estradiol levels ( $\pm$  SEM) being significantly lower

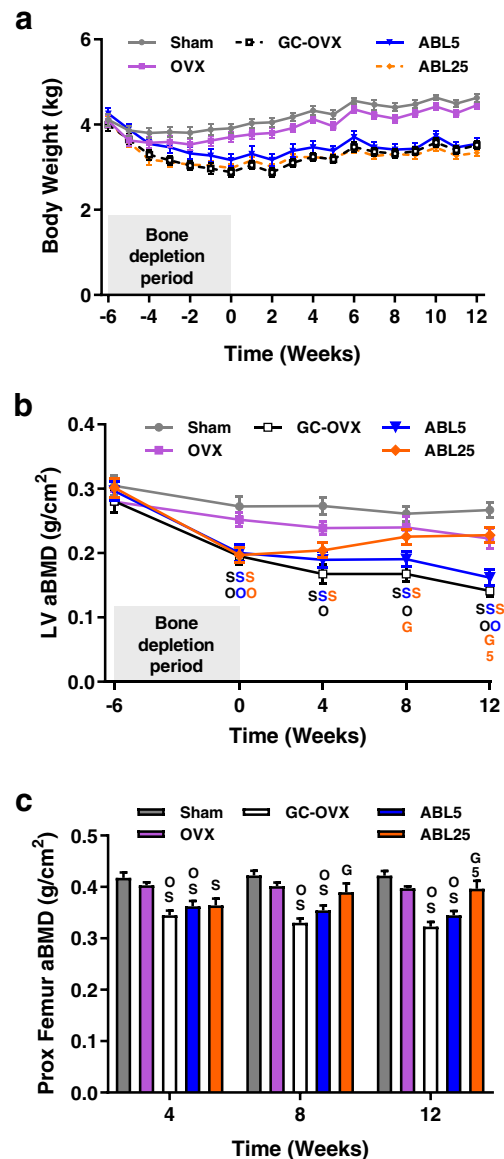


**Fig. 2** a Body weight and areal BMD data for the b L2-L5 lumbar vertebrae (LV) and c proximal femur. Data represent means  $\pm$  SEM, *n* = 7–8/group. OVX, ovariectomy; GC, glucocorticoid; ABL5, abaloparatide 5  $\mu$ g/kg/day; ABL25, abaloparatide 25  $\mu$ g/kg/day. Statistical comparisons of body weight data are in Results. For b, c, <sup>S</sup>*P* < 0.05 vs. sham, <sup>O</sup>*P* < 0.05 vs. OVX, <sup>G</sup>*P* < 0.05 vs. GC-OVX, and <sup>5</sup>*P* < 0.05 vs. ABL5 by two-way ANOVA and Tukey's post-test. For b, the color of statistical symbols indicates groups that differ from the symbol's alpha/numeric reference, i.e., a blue S indicates that the sham group differs from the ABL5 group

in the OVX group ( $20.9 \pm 1.5$  pmol/L) versus sham controls ( $41.4 \pm 4.7$  pmol/L; *P* < 0.001).

### DXA

LV aBMD was significantly lower in the GC-OVX group compared with sham and OVX groups at weeks 0, 4, 8, and 12 of the treatment period (Fig. 2b). LV aBMD was

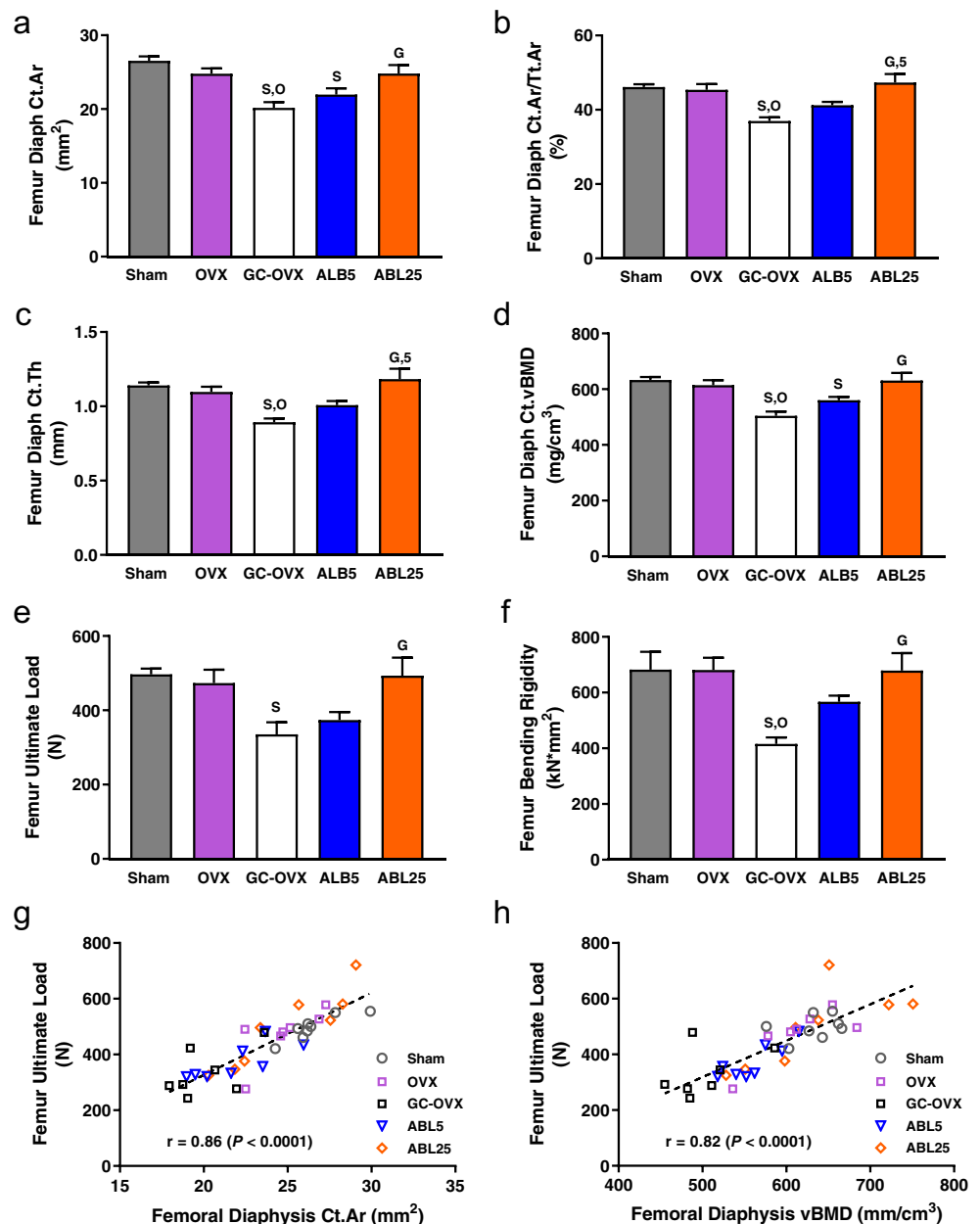
significantly higher in the ABL25 group compared with GC-OVX controls at weeks 8 and 12 (Fig. 2b). The proximal femur of the GC-OVX and ABL5 groups showed significantly lower aBMD compared with sham controls and OVX controls throughout the treatment period, and the ABL25 group exhibited significantly higher proximal femur aBMD at weeks 8 and 12 compared with GC-OVX controls (Fig. 2c).

## Micro-CT

Micro-CT data indicated that the femoral diaphysis of the GC-OVX group had lower Ct.Ar, Ct.Ar/Tt.Ar, Ct.Th, and Ct.vBMD (Fig. 3a–d) and higher Ct.Po (Table 1) compared

with the sham and OVX groups (all  $P < 0.05$ ). Higher Ct.Po in the GC-OVX group versus sham controls is evident in the representative reconstructed micro-CT images of the mid-femur and mid-sagittal distal femur shown in Fig. 4. The ABL25 group had greater Ct.Ar, Ct.Ar/Tt.Ar, Ct.Th, and Ct.vBMD versus GC-OVX controls (all  $P < 0.05$ ; Fig. 3a–d). Ct.TMD was significantly lower in the ABL25 group versus sham controls (Table 1). The distal femur of the GC-OVX group had lower Tb.N and higher SMI compared with sham controls, and the GC-OVX group also had lower Tb.BV/TV, Tb.vBMD, and Tb.Th compared with the sham and OVX groups (all  $P < 0.05$ ; Table 1). The ABL25 group had higher Tb.BV/TV and Tb.vBMD and lower SMI compared with GC-

**Fig. 3** Femur diaphysis micro-CT (a–d), biomechanics (e, f), and femoral diaphyseal bone mass-strength relationships (g–h). **a** Cortical area; **b** cortical area per total area; **c** cortical thickness; **d** cortical volumetric BMD; **e** ultimate load; **f** bending rigidity; **g**, **h** linear regressions for ultimate load vs micro-CT-derived cortical area and volumetric BMD, respectively. Additional femur diaphysis micro-CT data are presented in Table 1. Data represent means  $\pm$  SEM,  $n = 7$ –8/group. OVX, ovariectomy; GC, glucocorticoid (methyl-prednisolone); ABL5, abaloparatide 5  $\mu\text{g}/\text{kg}/\text{day}$ ; ABL25, abaloparatide 25  $\mu\text{g}/\text{kg}/\text{day}$ . <sup>S</sup> $P < 0.05$  vs. sham, <sup>O</sup> $P < 0.05$  vs. OVX, <sup>G</sup> $P < 0.05$  vs. GC-OVX, and <sup>5</sup> $P < 0.05$  vs. ABL5 by one-way ANOVA and Tukey's post-test



OVX controls (all  $P < 0.05$ ; Table 1). Improved distal femur trabecular architecture in the ABL25 group versus GC-OVX controls is evident in the representative micro-CT images of the distal femur trabecular ROI shown in Fig. 4.

The L4 vertebral body of the GC-OVX group had lower Tb.vBMD and Tb.Th compared with sham controls, and the ABL25 group had significantly higher Tb.BV/TV and Tb.vBMD compared with GC-OVX controls (all  $P < 0.05$ ; Table 1). Representative micro-CT images of the L4 trabecular region for the five groups are depicted in Fig. 4. The entire cross-section of the L4 vertebral body showed lower BV, BV/TV, vBMD, and TMD for the GC-OVX group compared with sham controls (all  $P < 0.05$ ), and there were no differences for these parameters between the GC-OVX, ABL5, and ABL25 groups (Table 1).

## Bone biomechanics

Destructive 3-point bending tests of the femoral diaphysis indicated lower ultimate load and bending rigidity in the GC-OVX group compared with sham controls, and the ABL25 group had higher ultimate load and bending rigidity compared with GC-OVX controls (all  $P < 0.05$ ; Fig. 3e–f). Femoral diaphyseal work to ultimate load was similar in all groups, with mean values in mJ ( $\pm$  SEM) as follows: sham,  $256.9 \pm 21.24$ ; OVX,  $333 \pm 59.30$ ; GC-OVX,  $306.6 \pm 89.46$ ; ABL5,  $294.3 \pm 49.67$ ; ABL25,  $437.0 \pm 87.55$ . Femoral diaphyseal ultimate load was highly correlated with micro-CT-derived femoral cortical area across all five groups ( $r = 0.86$ ,  $P < 0.0001$ ), as well as within the individual ABL5 group ( $r = 0.77$ ,  $P = 0.025$ ).

**Table 1** Micro-CT data for bones collected at the end of the treatment period. Additional femoral diaphysis micro-CT data are presented in Fig. 3. Data represent means  $\pm$  SEM,  $n = 7$ –8/group

	Sham	OVX	GC-OVX	ABL5	ABL25
<i>Femoral diaphysis</i>					
Tt.Ar (mm <sup>2</sup> )	57.59 $\pm$ 1.37	54.81 $\pm$ 1.50	54.82 $\pm$ 2.65	53.31 $\pm$ 1.82	52.59 $\pm$ 1.44
Ma.Ar (mm <sup>2</sup> )	30.98 $\pm$ 1.00	29.94 $\pm$ 1.48	32.62 $\pm$ 2.01	29.78 $\pm$ 1.54	26.64 $\pm$ 1.56
TMD (mg/cm <sup>3</sup> )	1285.8 $\pm$ 4.5	1275.8 $\pm$ 7.0	1267.8 $\pm$ 8.5	1270.6 $\pm$ 7.7	1253.4 $\pm$ 4.3 <sup>S</sup>
Ct.Po (%)	0.50 $\pm$ 0.04	0.43 $\pm$ 0.03	9.75 $\pm$ 3.61 <sup>S,O</sup>	7.27 $\pm$ 2.09	4.60 $\pm$ 0.82
<i>Distal femur</i>					
Tb.BV/TV (%)	35.81 $\pm$ 1.38	30.70 $\pm$ 1.09	24.34 $\pm$ 1.65 <sup>S,O</sup>	28.66 $\pm$ 1.38 <sup>S</sup>	31.15 $\pm$ 1.41 <sup>G</sup>
Tb.vBMD (mg/cm <sup>3</sup> )	368.5 $\pm$ 12.6	319.2 $\pm$ 11.2	258.8 $\pm$ 17.2 <sup>S,O</sup>	301.3 $\pm$ 12.8 <sup>S</sup>	325.1 $\pm$ 13.1 <sup>G</sup>
Tb.N (1/mm)	2.38 $\pm$ 0.11	2.11 $\pm$ 0.10	1.89 $\pm$ 0.11 <sup>S</sup>	2.09 $\pm$ 0.10	2.22 $\pm$ 0.12
Tb.Th (mm)	0.188 $\pm$ 0.003	0.168 $\pm$ 0.004	0.140 $\pm$ 0.004 <sup>S,O</sup>	0.157 $\pm$ 0.009 <sup>S</sup>	0.160 $\pm$ 0.006 <sup>S</sup>
Tb.Sp (mm)	0.477 $\pm$ 0.021	0.522 $\pm$ 0.031	0.552 $\pm$ 0.042	0.506 $\pm$ 0.026	0.493 $\pm$ 0.024
SMI	−0.09 $\pm$ 0.09	0.04 $\pm$ 0.05	0.36 $\pm$ 0.080 <sup>S</sup>	0.16 $\pm$ 0.07	−0.01 $\pm$ 0.09 <sup>G</sup>
Conn.D (1/mm <sup>3</sup> )	10.89 $\pm$ 0.71	10.19 $\pm$ 0.85	11.81 $\pm$ 0.91	11.61 $\pm$ 1.03	12.80 $\pm$ 1.06
<i>L4 trabecular bone</i>					
Tb.BV/TV (%)	22.20 $\pm$ 1.58	19.11 $\pm$ 1.67	16.50 $\pm$ 1.02	16.88 $\pm$ 0.72	23.94 $\pm$ 1.83 <sup>G,5</sup>
Tb.vBMD (mg/cm <sup>3</sup> )	266.8 $\pm$ 14.5	232.1 $\pm$ 15.1	197.9 $\pm$ 11.3 <sup>S</sup>	206.4 $\pm$ 7.2 <sup>S</sup>	279.7 $\pm$ 16.7 <sup>G,5</sup>
Tb.N (1/mm)	1.88 $\pm$ 0.11	1.75 $\pm$ 0.11	1.71 $\pm$ 0.06	1.81 $\pm$ 0.10	2.08 $\pm$ 0.14
Tb.Th (mm)	0.127 $\pm$ 0.005	0.116 $\pm$ 0.005	0.104 $\pm$ 0.003 <sup>S</sup>	0.103 $\pm$ 0.004 <sup>S</sup>	0.124 $\pm$ 0.005
Tb.Sp (mm)	0.557 $\pm$ 0.031	0.587 $\pm$ 0.036	0.583 $\pm$ 0.022	0.568 $\pm$ 0.038	0.508 $\pm$ 0.036
<i>L4 vertebral body</i>					
BV (mm <sup>3</sup> )	217.7 $\pm$ 10.8	188.2 $\pm$ 10.0	165.8 $\pm$ 8.9 <sup>S</sup>	174.1 $\pm$ 11.6	192.5 $\pm$ 13.6
TV (mm <sup>3</sup> )	557.7 $\pm$ 25.5	493.8 $\pm$ 16.0	547.8 $\pm$ 24.8	558.7 $\pm$ 24.8	544.2 $\pm$ 21.8
BV/TV (%)	39.21 $\pm$ 1.62	38.10 $\pm$ 1.47	30.36 $\pm$ 0.85 <sup>S,O</sup>	31.02 $\pm$ 1.02 <sup>S,O</sup>	35.18 $\pm$ 1.42
vBMD (mg/cm <sup>3</sup> )	415.9 $\pm$ 15.7	399.6 $\pm$ 13.8	316.4 $\pm$ 8.5 <sup>S,O</sup>	327.3 $\pm$ 28.0 <sup>S,O</sup>	368.8 $\pm$ 13.6
TMD (mg/cm <sup>3</sup> )	938.3 $\pm$ 4.9	936.0 $\pm$ 2.9	907.9 $\pm$ 3.5 <sup>S,O</sup>	916.6 $\pm$ 6.8 <sup>S</sup>	907.3 $\pm$ 5.6 <sup>S,O</sup>

<sup>S</sup>  $P < 0.05$  vs. sham

<sup>O</sup>  $P < 0.05$  vs. OVX

<sup>G</sup>  $P < 0.05$  vs. GC-OVX

<sup>5</sup>  $P < 0.05$  vs ABL5

OVX ovariectomy, GC glucocorticoid, ABL5 abaloparatide 5  $\mu$ g/kg/day, ABL25 abaloparatide 25  $\mu$ g/kg/day, Tt total, Ar area, Ma marrow, TMD tissue mineral density, Ct cortical, Po porosity, Tb trabecular, BV bone volume, TV total volume, vBMD volumetric bone mineral density, N number, Th thickness, Sp separation, SMI structure model index, Conn.D connectivity density

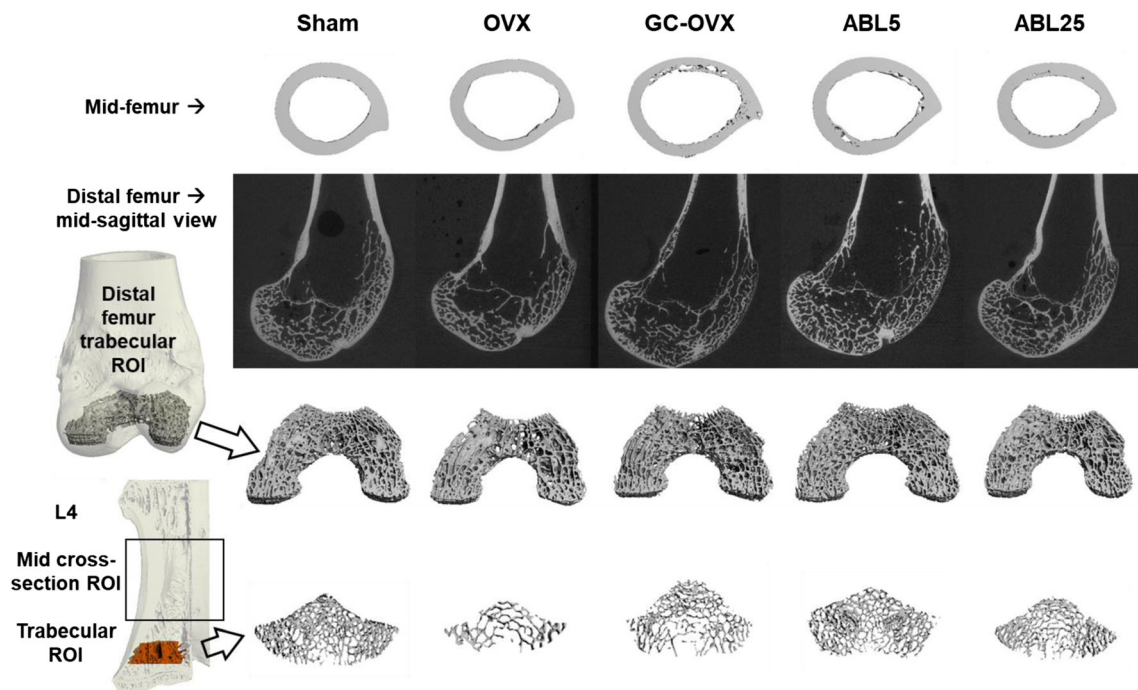


**Fig. 4** Micro-CT regions of interest (ROIs) and representative reconstructed images. L4, 4th lumbar vertebra; OVX, ovariectomized; GC, glucocorticoid (methyl-prednisolone); ABL5, abaloparatide 5  $\mu\text{g}/\text{kg}/\text{day}$ ; ABL25, abaloparatide 25  $\mu\text{g}/\text{kg}/\text{day}$

and the ABL25 group ( $r = 0.92$ ,  $P = 0.001$ ) (Fig. 3g). Femoral diaphyseal ultimate load also correlated with femoral diaphyseal Ct.vBMD across all groups ( $r = 0.82$ ,  $P < 0.0001$ ) and within the ABL5 group ( $r = 0.84$ ,  $P = 0.009$ ) and the ABL25 group ( $r = 0.76$ ,  $P = 0.03$ ) (Fig. 3h). Femoral Ct.Th was also a strong predictor of ultimate load (overall  $r$  value of 0.87,  $P < 0.0001$ ; regression not shown).

Destructive compression testing of L4 showed lower ultimate load and work to ultimate load in the GC-OVX group versus sham controls (both  $P < 0.05$ ; Table 2). There were no significant differences between the GC-OVX, ABL5, and ABL25 groups for ultimate load, stiffness, or work to ultimate load (Table 2). Linear regression analyses indicated that L4 ultimate load best correlated with L4 total vBMD, with an overall  $r$  value of 0.82 ( $P < 0.0001$ ) and  $r$  values of 0.71 ( $P = 0.05$ ) and 0.75 ( $P = 0.03$ ) for the ABL5 and ABL25 groups, respectively (regressions not shown).

**Table 2** Bone biomechanics for the L4 vertebral body at the end of the treatment period. Data represent means  $\pm$  SEM,  $n = 7$ –8/group

	Sham	OVX	GC-OVX	ABL5	ABL25
Ultimate load (N)	1388 $\pm$ 89	1256 $\pm$ 77	894 $\pm$ 69 <sup>S</sup>	1045 $\pm$ 106	1095 $\pm$ 91
Stiffness (N/mm)	6236 $\pm$ 938	6910 $\pm$ 252	4860 $\pm$ 336	5400 $\pm$ 689	6309 $\pm$ 514
Work to ult load (mJ)	262.4 $\pm$ 20.9	193.1 $\pm$ 21.2	131.3 $\pm$ 18.3 <sup>S</sup>	175.9 $\pm$ 26.6 <sup>S</sup>	153.4 $\pm$ 14.2 <sup>S</sup>

<sup>S</sup>  $P < 0.05$  vs. sham

N newton, mJ millijoule, OVX ovariectomy, GC glucocorticoid, ABL5 abaloparatide 5  $\mu\text{g}/\text{kg}/\text{day}$ , ABL25 abaloparatide 25  $\mu\text{g}/\text{kg}/\text{day}$

## Discussion

Glucocorticoids play an important role in alleviating inflammation-related symptoms and morbidity in a variety of rheumatic diseases and other inflammatory disorders. Unfortunately, GC therapies can also reduce bone mass by suppressing bone formation and increasing bone resorption, leading to reduced bone strength that can increase fracture risk [1, 2, 22]. Beyond the adverse effects of GCs on bone, the underlying inflammation for which GCs are often prescribed can also adversely affect the balance of bone formation and resorption, further contributing to rapid bone loss in individuals receiving GCs [1]. GCs may also impair bone matrix strength (bone quality) independent of their effects on bone mass and can also increase the risk of falls [1], providing further rationales for administering bone-targeted therapies to strengthen the skeleton of at-risk patients on GC therapy.

GCs cause substantial bone loss in rabbits [23] by reducing bone formation and increasing bone resorption [24]. Unlike mice and rats, rabbits undergo physiological intracortical remodeling [25], an important feature for non-clinical GIOP studies because GCs tend to increase cortical porosity in humans [5], as they do in rabbits [25]. Rabbits are therefore considered suitable by the US Food and Drug Administration (FDA) for the non-clinical evaluation of candidate GIOP therapies [26]. The current study assessed the effects of the osteoanabolic PTHrP analog abaloparatide on bone mass and strength in GC-challenged OVX rabbits. This combined estrogen deficiency plus GC model was developed in part because of the narrow window between minimal GC doses that cause bone loss in rabbits versus doses that cause significant morbidity and mortality [23, 24]. Moderate GC doses or OVX alone are generally insufficient to create significant osteopenia in rabbits, but the combination of OVX with moderate GC doses induces significant osteopenia in rabbits within 6 weeks [23, 25, 27]. The current study corroborates those findings in showing no significant vertebral BMD deficits in the OVX group but significant deficits in the GC-OVX group within 6 weeks of GC exposure compared with sham controls. After a total of 18 weeks, the GC-OVX group also had deficits in vertebral and distal femoral trabecular bone volume, density, and architecture, reductions in femoral diaphyseal bone volume, cortical thickness, and density, and lower vertebral and femoral diaphyseal bending strength compared with sham controls. Abaloparatide treatment initiated after 6 weeks of OVX plus GC exposure led to substantial improvements in cortical and trabecular bone at the 25 µg/kg/day dose compared with GC-OVX controls, with no significant treatment effects observed for the 5 µg/kg/day dose.

The ABL25 group showed complete normalization of GC-OVX-associated reductions in femoral diaphyseal cortical thickness and vBMD, and linear regression analyses suggest that those treatment effects contributed to normalization of femoral diaphyseal bending strength and rigidity observed with the higher abaloparatide dose. Mechanistically, improved femoral diaphyseal thickness and vBMD in the ABL25 group may be best explained by abaloparatide effects on the endocortical and intracortical envelopes: there was no evidence for increased periosteal apposition in the ABL25 group based on femoral diaphyseal Tt.Ar results, whereas the ABL25 group showed a trend toward reduced marrow area (a proxy for increased endocortical apposition), with a relative reduction of 4% vs GC-OVX controls ( $P = 0.07$ ), and a non-significant relative reduction in cortical porosity of 53% vs GC-OVX controls ( $P = 0.30$ ). The Ct.Po results for the ABL25 group may be reassuring because patients receiving GC therapy can show increased cortical porosity [5], as did the GC-OVX group in the current study, and PTH receptor agonists can increase long bone cortical porosity in non-GC-challenged rabbits [28, 29].

Trabecular bone responses to abaloparatide included higher BV/TV and vBMD and lower SMI at the distal femur of the ABL25 group versus GC-OVX controls. Lower SMI in the ABL25 group suggests improved trabecular micro-architecture, with more plate-like rather than rod-like trabecular elements. The L4 vertebral body of the ABL25 group also showed higher trabecular BV/TV and vBMD compared with GC-OVX controls. However, neither abaloparatide group showed significant differences versus GC-OVX controls for micro-CT variables assessed through the entire mid-region of the vertebral body (illustrated in Fig. 4), which aligns with a lack of significant increases in L4 vertebral strength in the abaloparatide groups. Regression analyses indicated that abaloparatide treatment did not alter mass-strength relationships for L4, which reconciles modestly higher L4 BV/TV and vBMD in the ABL25 group (+16% versus GC-OVX controls) with modestly higher L4 ultimate load (+18%) and stiffness (+30%).

This study has several limitations. The OVX state of the GC-challenged rabbits limits interpretations of how abaloparatide might affect GIOP in estrogen-replete states. The effects of abaloparatide in GC-treated male rabbits remains unknown, though abaloparatide significantly improves cortical and trabecular bone mass and architecture in hypogonadal male rats [19] as it does in hypogonadal female rats [15–17]. The effect of abaloparatide on hip and femoral neck strength in GIOP settings is another important unanswered question that might be best addressed in other species, as the rabbit proximal femur lacks a distinct femoral neck for biomechanical testing [30]. The effects of abaloparatide on vertebral strength in GC-challenged animals might also warrant testing in other species; compared with humans, monkeys and rodents, vertebral bodies of rabbits are long and narrow with minimal trabecular bone [30]. Abaloparatide consistently increases vertebral strength in GC-naïve rats and monkeys [15, 16, 18], and abaloparatide reduces vertebral fracture risk by 86% versus placebo in women with postmenopausal osteoporosis [13], though that trial excluded subjects who took daily oral GCs within the previous 12 months. The lack of bone histomorphometry and bone turnover marker data limits insights regarding possible mechanisms by which GC + OVX reduced bone mass and strength and abaloparatide improved bone mass and strength, though previous animal studies cited above indicate the common abaloparatide effect of increasing bone formation without increasing bone resorption.

In summary, GC-challenged OVX rabbits exhibited significant deficits in trabecular and cortical bone mass, leading to reduced vertebral and femoral diaphyseal strength. Twelve weeks of abaloparatide therapy initiated after 6 weeks of bone loss and throughout ongoing GC administration led to increases in trabecular bone volume and density and improved trabecular microarchitecture. Abaloparatide administration also increased cortical bone volume and density and improved

femoral diaphyseal bending strength. These results provide preliminary preclinical support for abaloparatide as an investigational therapy for improving BMD and bone strength in settings where GC therapy causes meaningful bone loss and an elevated risk of fractures.

**Acknowledgements** Medical writing support was provided by Paul J. Kostenuik, PhD, through Phylon Pharma Services. The authors would like to thank Jordan Nustad and Jiayi Ma for assisting with the micro-CT and biomechanical testing and Danfeng Liu, Mei-Shu Shih, and Yuan Hongjiang from PharmaLegacy, for their oversight of the in-life portion of the study.

## Compliance with ethical standards

**Conflicts of interest** Funding for this work was provided by Radius Health. HKC, GH, and BL are current or former employees of Radius Health.

**Open Access** This article is distributed under the terms of the Creative Commons Attribution-NonCommercial 4.0 International License (<http://creativecommons.org/licenses/by-nc/4.0/>), which permits any noncommercial use, distribution, and reproduction in any medium, provided you give appropriate credit to the original author(s) and the source, provide a link to the Creative Commons license, and indicate if changes were made.

## References

- Briot K, Roux C (2015) Glucocorticoid-induced osteoporosis. *RMD Open* 1(1):e000014
- Canalis E, Mazziotti G, Giustina A, Bilezikian JP (2007) Glucocorticoid-induced osteoporosis: pathophysiology and therapy. *Osteoporos Int* 18(10):1319–1328
- Chappard D, Josselin N, Rouge-Maillart C, Legrand E, Basle MF, Audran M (2007) Bone microarchitecture in males with corticosteroid-induced osteoporosis. *Osteoporos Int* 18(4):487–494
- Piemontese M, Xiong J, Fujiwara Y, Thostenson JD, O'Brien CA (2016) Cortical bone loss caused by glucocorticoid excess requires RANKL production by osteocytes and is associated with reduced OPG expression in mice. *Am J Physiol Endocrinol Metab* 311(3):E587–E593
- Vedi S, Elkin SL, Compston JE (2005) A histomorphometric study of cortical bone of the iliac crest in patients treated with glucocorticoids. *Calcif Tissue Int* 77(2):79–83
- Martin TJ (2005) Osteoblast-derived PTHrP is a physiological regulator of bone formation. *J Clin Invest* 115(9):2322–2324
- Miao D, He B, Jiang Y, Kobayashi T, Sorocéanu MA, Zhao J, Su H, Tong X, Amizuka N, Gupta A, Genant HK, Kronenberg HM, Goltzman D, Karaplis AC (2005) Osteoblast-derived PTHrP is a potent endogenous bone anabolic agent that modifies the therapeutic efficacy of administered PTH 1-34. *J Clin Invest* 115(9):2402–2411
- Walsh CA, Birch MA, Fraser WD, Lawton R, Dorgan J, Walsh S, Sansom D, Beresford JN, Gallagher JA (1995) Expression and secretion of parathyroid hormone-related protein by human bone-derived cells in vitro: effects of glucocorticoids. *J Bone Miner Res* 10(1):17–25
- Ahlstrom M, Pekkinen M, Lamberg-Allardt C (2009) Dexamethasone downregulates the expression of parathyroid hormone-related protein (PTHrP) in mesenchymal stem cells. *Steroids* 74(2):277–282
- de Castro LF, Lozano D, Dapia S, Portal-Nunez S, Caeiro JR, Gomez-Barrena E, Esbrit P (2010) Role of the N- and C-terminal fragments of parathyroid-hormone-related protein as putative therapies to improve bone regeneration under high glucocorticoid treatment. *Tissue Eng Part A* 16(4):1157–1168
- Saag KG, Zanchetta JR, Devogelaer JP, Adler RA, Eastell R, See K, Kregge JH, Krohn K, Warner MR (2009) Effects of teriparatide versus alendronate for treating glucocorticoid-induced osteoporosis: thirty-six-month results of a randomized, double-blind, controlled trial. *Arthritis Rheum* 60(11):3346–3355
- Bostrom MP, Gamradt SC, Asnis P, Vickery BH, Hill E, Avnur Z, Waters RV (2000) Parathyroid hormone-related protein analog RS-66271 is an effective therapy for impaired bone healing in rabbits on corticosteroid therapy. *Bone* 26(5):437–442
- Miller PD, Hattersley G, Riis BJ, Williams GC, Lau E, Russo LA, Alexandersen P, Zerbini CAF, Hu MY, Harris AG, Fitzpatrick LA, Cosman F, Christiansen C, for the ACTIVE Study Investigators (2016) Effect of abaloparatide vs placebo on new vertebral fractures in postmenopausal women with osteoporosis: a randomized clinical trial. *JAMA* 316(7):722–733
- Cosman F, Miller PD, Williams GC, Hattersley G, Hu MY, Valter I, Fitzpatrick LA, Riis BJ, Christiansen C, Bilezikian JP, Black D (2017) Eighteen months of treatment with subcutaneous abaloparatide followed by 6 months of treatment with alendronate in postmenopausal women with osteoporosis: Results of the ACTIVEExtend trial. *Mayo Clin Proc* 92(2):200–210
- Bahar H, Gallacher K, Downall J, Nelson CA, Shomali M, Hattersley G (2016) Six weeks of daily abaloparatide treatment increased vertebral and femoral bone mineral density, microarchitecture and strength in ovariectomized osteopenic rats. *Calcif Tissue Int* 99(5):489–499
- Varela A, Chouinard L, Lesage E, Guldberg R, Smith SY, Kostenuik PJ, Hattersley G (2017) One year of abaloparatide, a selective peptide activator of the PTH1 receptor, increased bone mass and strength in ovariectomized rats. *Bone* 95:143–150
- Varela A, Chouinard L, Lesage E, Smith SY, Hattersley G (2017) One year of abaloparatide, a selective activator of the PTH1 receptor, increased bone formation and bone mass in osteopenic ovariectomized rats without increasing bone resorption. *J Bone Miner Res* 32(1):24–33
- Doyle N, Varela A, Haile S, Guldberg R, Kostenuik PJ, Ominsky MS, Smith SY, Hattersley G (2018) Abaloparatide, a novel PTH receptor agonist, increased bone mass and strength in ovariectomized cynomolgus monkeys by increasing bone formation without increasing bone resorption. *Osteoporos Int* 29(3):685–697
- Chandler H, Lanske B, Varela A, Guillot M, Boyer M, Brown J, Pierce A, Ominsky M, Mitlak B, Baron R, Kostenuik P, Hattersley G (2019) Abaloparatide, a novel osteoanabolic PTHrP analog, increases cortical and trabecular bone mass and architecture in ovariectomized rats by increasing bone formation without increasing bone resorption. *Bone* 120:148–155
- Bouxein ML, Boyd SK, Christiansen BA, Guldberg RE, Jepsen KJ, Muller R (2010) Guidelines for assessment of bone microstructure in rodents using micro-computed tomography. *J Bone Miner Res* 25(7):1468–1486
- Cacchioli A, Ravanetti F, Soliani L, Borghetti P (2012) Preliminary study on the mineral apposition rate in distal femoral epiphysis of New Zealand white rabbit at skeletal maturity. *Anat Histol Embryol* 41(3):163–169
- Mawatari T, Miura H, Hamai S, Shuto T, Nakashima Y, Okazaki K, Kinukawa N, Sakai S, Hoffmann PF, Iwamoto Y, Keaveny TM (2008) Vertebral strength changes in rheumatoid arthritis patients treated with alendronate, as assessed by finite element analysis of

- clinical computed tomography scans: a prospective randomized clinical trial. *Arthritis Rheum* 58(11):3340–3349
23. Castaneda S, Calvo E, Largo R, Gonzalez-Gonzalez R, de la Piedra C, Diaz-Curiel M, Herrero-Beaumont G (2008) Characterization of a new experimental model of osteoporosis in rabbits. *J Bone Miner Metab* 26(1):53–59
  24. Eberhardt AW, Yeager-Jones A, Blair HC (2001) Regional trabecular bone matrix degeneration and osteocyte death in femora of glucocorticoid-treated rabbits. *Endocrinology* 142(3):1333–1340
  25. Baofeng L, Zhi Y, Bei C, Guolin M, Qingshui Y, Jian L (2010) Characterization of a rabbit osteoporosis model induced by ovariectomy and glucocorticoid. *Acta Orthop* 81(3):396–401
  26. FDA (2016) Osteoporosis: nonclinical evaluation of drugs intended for treatment. Guidance for industry. US Department of Health and Human Services, Food and Drug Administration, Center for Drug Evaluation and Research (CDER) <http://www.fda.gov/downloads/Drugs/GuidanceComplianceRegulatoryInformation/Guidances/UCM506366.pdf>
  27. Almagro MI, Roman-Blas JA, Bellido M, Castaneda S, Cortez R, Herrero-Beaumont G (2013) PTH [1-34] enhances bone response around titanium implants in a rabbit model of osteoporosis. *Clin Oral Implants Res* 24(9):1027–1034
  28. Hirano T, Burr DB, Cain RL, Hock JM (2000) Changes in geometry and cortical porosity in adult, ovary-intact rabbits after 5 months treatment with LY333334 (hPTH 1-34). *Calcif Tissue Int* 66(6):456–460
  29. Yamane H, Takakura A, Shimadzu Y, Kodama T, Lee JW, Isogai Y, Ishizuya T, Takao-Kawabata R, Iimura T (2017) Acute development of cortical porosity and endosteal naive bone formation from the daily but not weekly short-term administration of PTH in rabbit. *PLoS One* 12(4):e0175329
  30. Bagi CM, Berryman E, Moalli MR (2011) Comparative bone anatomy of commonly used laboratory animals: implications for drug discovery. *Comp Med* 61(1):76–85

**Publisher's note** Springer Nature remains neutral with regard to jurisdictional claims in published maps and institutional affiliations.